Sensors and Actuators B 136 (2009) 350–358

Contents lists available at ScienceDirect

Sensors and Actuators B: Chemical

journal homepage: www.elsevier.com/locate/snb

Multiplexed electrical sensor arrays in microfluidic networks

Matthew C. Cole, Paul J.A. Kenis*

University of Illinois at Urbana-Champaign, Department of Chemical & Biomolecular Engineering, 600 S. Mathews Ave, Urbana, IL 61801, USA

ARTICLE INFO

Article history:
Received 3 July 2008
Received in revised form
23 November 2008
Accepted 8 December 2008
Available online 14 December 2008

Keywords:
Multiplexing
Microfluidic sensing
Electrical sensors
Sensor arrays

ABSTRACT

A major limitation of many microfluidic platforms is their inability to perform large scale, real time, sensing, routing, or scheduling of the materials moving through them. This paper seeks to address the first of these deficiencies by introducing a multiplexed sensing architecture capable of monitoring the movement of liquid droplets in large microfluidic networks. We describe the design and fabrication of the sensor array, as well as its integration and testing in microfluidic networks. Individual sensors consisting of small electrical components (resistors, capacitors, or conduction gaps) are addressed using a multiplexing approach that allows an array of $m \times n$ sensors to be supported by only $m+n+1$ electrical contacts, as compared to the $2 \times m \times n$ contacts traditionally necessary. For example, a multiplexed 10×10 array of sensors can be operated with 21 contacts, as opposed to the 200 contacts needed in a traditional configuration. The multiplexing relies on the fact that each sensing element is connected to two electrical leads, and each electrical lead is connected to multiple sensing elements. Here we show the principle using a 4×4 multiplexed arrays of resistive and capacitive sensors to monitor the passage of discrete liquid plugs through a microfluidic network.

1. Introduction

As microfluidic devices continue to decrease in size and increase in complexity, the ability to monitor the passage of material through them becomes ever more important. In recent years, microfluidic systems have been used in many chemical and biological applications, including: DNA analysis [1], capillary electrophoresis [2], cell cytometry [3], high throughput screening for combinatorial chemistry [4], fuel cells [5], combining multiple biological assays onto a single chip [6], and the generation of multistream segmented flow regimes [7]. However, as impressive as these microchemical systems are, during operation one typically has little to no exact information about the position and speed of material moving through them. This inability to monitor and control the position of discrete liquid elements becomes a significant issue when scaling up from microfluidic configurations with only a few channels to configurations comprised of extensive channel networks designed for the high throughput processing of multiple droplets flowing within a carrier stream. For microfluidic devices to continue to evolve, better real time routing and scheduling methods are needed. Such a control system will depend on the ability to detect the position of material throughout a microfluidic network using an array of appropriate sensors [8]. Ideally, the sensors used should be easy to fabricate and integrate with current microfluidic devices, require a small footprint of space within the device, and consume only a small amount of power.

Numerous reports and reviews have appeared in the literature on various types of sensing in microfluidic devices. Optical detection techniques based on fluorescence [9,10], absorbance [9,10], luminescence [11], and waveguides [12,13] are the most prevalent. Others have used some form of electrochemical detection during electrophoretic separations, including amperometry [14–18], conductimetry [19–22], and potentiometry [22–24]. Still others have used electrical sensors such as resistors [25–28], capacitors [29–33], and conduction gaps [34–39] for the detection of specific chemical species or biological cells, or the measurement of certain fluid properties (e.g. concentration, temperature, or flow rate). These electrical sensing principles can also easily be applied to the detection of a discrete liquid element (e.g. in plug [40–42] or slug [43] flow regimes) at a specified position within a microfluidic network, which is the goal of this study [44].

In this work, we integrate arrays of multiplexed electrical sensors into microfluidic networks. Whereas most optical sensing methods rely on an external light source and detector, electrical sensors can be incorporated directly within a microfluidic device because of their inherent minimal thickness. Additionally, they are easy to fabricate by standard photolithographic techniques, and require only a small amount of power for operation. For the purposes of liquid droplet detection, a small constant current or potential is applied across a sensing element (either a resistor, capacitor, or conduction gap) patterned in a microchannel, and the corresponding output signal is continually monitored. A change in

* Corresponding author. Tel.: +1 217 265 0523.
E-mail address: kenis@illinois.edu (P.J.A. Kenis).

0925-4005/$ – see front matter © 2008 Elsevier B.V. All rights reserved.
doi:10.1016/j.snb.2008.12.010

the output signal indicates a change in a physical property (thermal conductivity, dielectric constant, or electrical conductivity, depending on the sensor type) of the liquid surrounding the sensor, thereby detecting when a liquid element arrives at or passes a certain point.

Scaling these individual sensors up into large arrays spanning an entire microfluidic network is logistically complex. As the number of sensors increases, the number of electrical leads necessary to connect the sensors with external monitoring equipment will also increase. This rapid growth renders the design, fabrication and, implementation of the sensor array exceedingly difficult. The creation of a large array of sensors that also minimizes the number of electrical leads necessary is therefore desirable. Previous work on creating arrays of similar sensors has resulted in either small arrays that are difficult to scale up [45–47], or complicated fabrication procedures [8]. Others have extensively characterized individual electrical sensors for microfluidic droplet position detection, yet have not reported on the possibility of scaling those sensors up into arrays [44]. Here we describe a fully scalable and planar sensor configuration that employs a multiplexing approach allowing an array of $m \times n$ sensors to be controlled by only $m+n+1$ electrical leads, as opposed to the usual $2 \times m \times n$, corresponding to 2 leads per sensor. We will discuss the design, fabrication and testing of resistive, capacitive, and conductive sensors in single channels, as well as 4×4 multiplexed arrays of resistive and capacitive sensors within microfluidic networks.

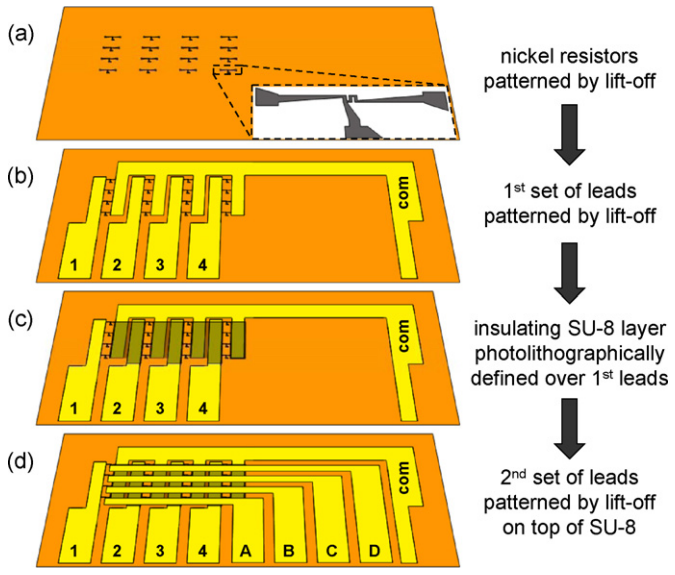

Fig. 2. Step-by-step fabrication procedure of a typical substrate with a 4×4 array of multiplexed resistive sensors. (a) Array of 80 nm thick nickel resistive sensors patterned by lift-off; (b) the first set of leads (vertical; no. 1–4) as well as the common lead (com), all 100-nm Au, patterned by lift-off; (c) insulating layer of 4-μm SU-8 photoresist, selectively patterned on top of the underlying first set of leads; (d) second set of leads (horizontal; no. A–D), 300-nm Au, patterned by lift-off.

2. Electrical sensing principles for microfluidics

2.1. Resistive sensing

The resistive sensors discussed here are thin-film serpentine resistors, similar to traditional resistive heaters used as flow and temperature sensors [25,48–51]. When a small constant potential is applied, the resistor quickly heats up to some constant temperature in proportion to its temperature coefficient of resistance (TCR) and the thermal conductivity of the surrounding liquid. When liquids of varying thermal conductivity flow over the resistor, the temperature of the resistor fluctuates correspondingly, resulting in changes to the overall resistance of the resistor, and thus to the output current. Therefore, a change in the liquid contacting the resistor is detected when the current through the resistor changes.

2.2. Capacitive sensing

The capacitive sensors used in this study consisted of two coplanar gold electrodes separated by a small gap [32], instead of the more common parallel plate capacitor geometry [33]. A coplanar geometry was used because it allows for a simpler microfabrication procedure than a parallel plate structure. Previous experimental and theoretical work has shown that the maximum capacitive signal in the coplanar configuration is obtained when the electrode gap spacing is minimized, and the exposed electrode width is comparable to the height of the channel surrounding them [32,52].

Most of these capacitive sensing elements are operated in an AC mode. A difference in capacitance is measured upon a change in liquid composition between the electrodes. *In contrast, we will operate our coplanar capacitive sensors in a constant potential mode, measuring a short induced current upon a change in liquid composition.* A small constant potential is applied across the gap between the electrodes and the current is monitored as a function of time. Equal and opposite charges build up on the ends of the electrodes and no change in current is detected until a liquid with a different dielectric constant passes over the sensor. The change in dielectric constant manifests itself a change in the charge distribution on

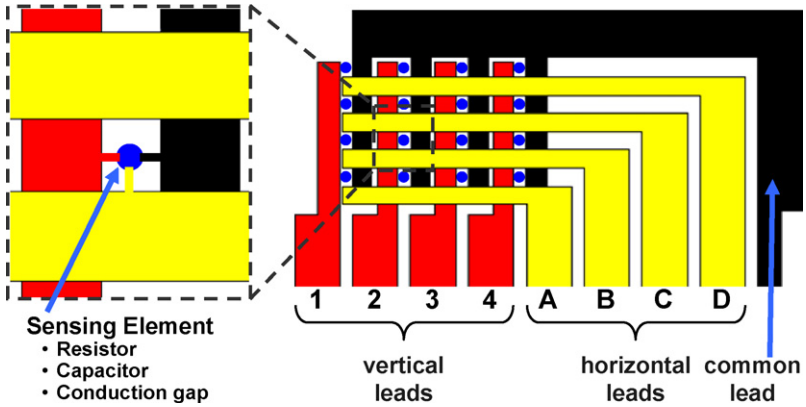

Fig. 1. Schematic illustrating the multiplexing detection principle, here in a 4×4 array of sensing elements (blue dots). Each sensing element (a resistor, a capacitor, or a conduction gap) is connected to two separate input leads (red and yellow) and one common output lead (black). Each lead is connected to multiple sensing elements. A unique combination of the responses from leads 1–4 and leads A–D pinpoints the location at which a sensing event, e.g. a change in liquid composition, takes place. (For interpretation of the references to color in this figure legend, the reader is referred to the web version of the article.)

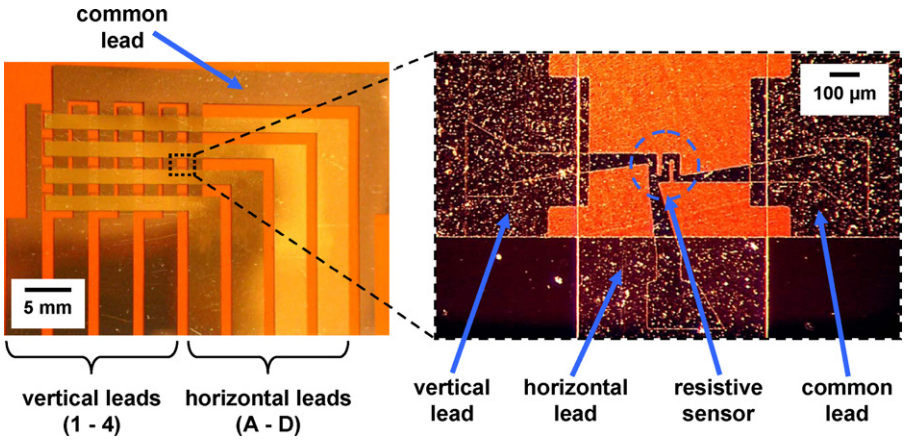

Fig. 3. Optical micrograph of a substrate with a multiplexed 4 × 4 array of resistive sensors. The enlarged view to the right shows an individual resistive sensing element, and the leads it is connected to. The horizontal leads cross over the vertical leads with an electrically insulating layer of SU-8 in between them.

the ends of the electrodes, leading to a sudden and sharp induced current spike.

Capacitive sensing based on an induced current is much simpler than AC-based capacitance detection methods. Whereas AC-based detection seeks to directly monitor exceedingly small fluctuations in the capacitance of a sensor (on the order of femto-Farads), the induced current method used here relies on relatively large changes in the current through the system (on the order of nano-Amperes). The small signals produced using AC methods generally require the use of complicated experimental setups, electrical shielding, and precise temperature control. AC capacitance bridges that can automatically overcome some of these problems and directly monitor changes in capacitance in real time are commercially available, but they are very expensive compared to the relatively simple low-voltage power supply used here [31,33].

2.3. Conductive sensing

As in the capacitive case, the conductive sensors used here consisted of two coplanar gold leads separated by a small gap, similar to prior work [36,37]. A small constant current is applied between the leads while the potential drop across the gap is monitored. When the fluid filling the gap is nonconductive, the system acts like an open circuit and the measured potential drop is infinite. When a conductive liquid fills the gap, the circuit is closed and a potential drop that is proportional to the conductivity of the liquid is detected. Liquids of different conductivity can thus also be easily distinguished.

3. Design, fabrication, and characterization of multiplexed arrays of electrical sensors

3.1. Design of multiplexed arrays of electrical sensors

The multiplexing principle implemented here relies on the fact that each sensing element is connected to two electrical leads, and each lead is connected to multiple sensors (Fig. 1). A given array of $m \times n$ sensors is comprised of (i) m vertical leads that are patterned first, (ii) n horizontal leads that are patterned second, and (iii) one output lead that is common to all the sensors. A thin insulating polymer layer prevents the overlapping leads from making direct electrical contact. Each sensor in the array is connected to a

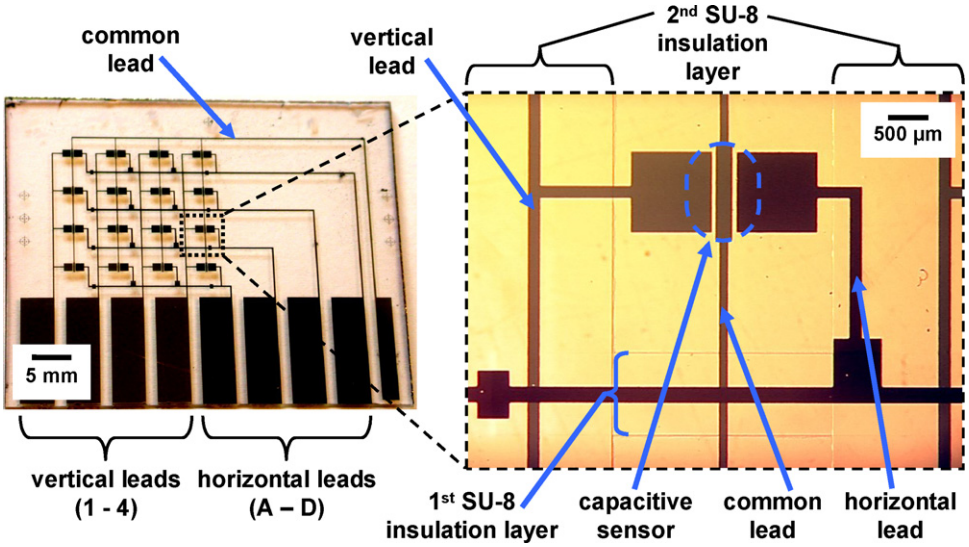

Fig. 4. Optical micrograph of a substrate with a multiplexed 4 × 4 array of capacitive sensors. The enlarged view to the right shows an individual capacitive sensing element, and the leads it is connected to. The vertical and horizontal leads overlap, but are separated from each other by an electrically insulating SU-8 layer. A second SU-8 layer insulates the exposed leads from the liquid flowing through the microfluidic network placed on top.

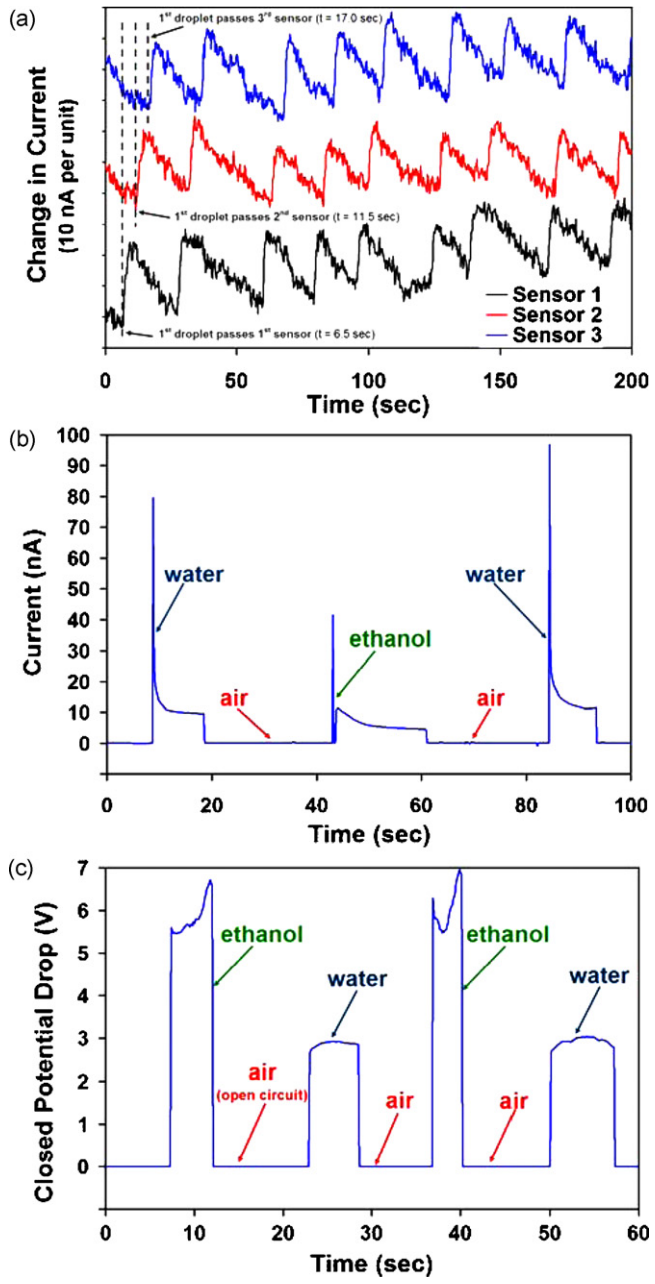

Fig. 5. Plug flow detection traces for individual electrical sensors: (a) a linear series of three individual resistive sensors spaced 4 mm apart in a microfluidic channel sequentially detecting alternating 5-μL plugs of water and FC-40. The three vertical dashed lines indicate the passage of the first water droplet over the first, second, and third sensors, at t = 6.5, 11.5, and 17.0 s, respectively. Each increase and decrease in current represents the passage of one plug of water and one plug of FC-40, respectively, over a resistor. The lag between peaks corresponds to the time a plug takes to travel from one sensor to the next, here flowing at a rate of approximately 0.1 cm/s. The slopes of the of water segments of the plot are much sharper than those of the FC-40 because water (κ_{water} = 0.6 W/m K) has a much high thermal conductivity that the FC-40 ($\kappa_{FC\text{-}40}$ = 0.06 W/m K), and therefore causes a much faster temperature change; (b) a single capacitive sensor detecting 5-μL water and ethanol plugs separated by air. Each new liquid plug causes a sharp induced current spike in proportion to the dielectric constant of the liquid, before leveling off to a nominal value depending on the conductivity of the liquid; (c) a single conductive sensor detecting 5-μL water and ethanol plugs separated by air. When a conductive liquid covers the sensing element, the circuit is closed and a potential drop proportional to the conductivity of the liquid is observed.

unique combination of one vertical lead and one horizontal lead, along with a connection to the common output. In this configuration, when a change in liquid occurs at a certain sensor (m,n), a change in the monitored output value is displayed in the trace of both lead m and lead n at the same time. This allows one to pinpoint exactly where a liquid element is in a microfluidic system with only $m+n+1$ leads, as opposed to the conventional case of having two separate leads for each sensing element, which would require $2 \times m \times n$ total leads. An array of 10×10 sensors, for example, would require 200 leads in a non-multiplexed configuration, whereas the multiplexed design proposed here requires only 21 leads for the same array, a reduction by a factor of nearly 5. Note that this reduction in complexity factor scales nonlinearly: For a 100×100 array, the corresponding numbers are 20,000 versus 201, an almost 100-fold reduction.

A fundamental difference between the multiplexed resistive system and a multiplexed capacitive system is that, in the resistive case, both of the leads for a given sensor element are connected to the *same* resistor. In the capacitive case, both leads cannot be connected to the same sensor gap, because that would short-circuit the array. Therefore, in order to achieve a multiplexed capacitive system, two completely separate leads are needed, each forming their own gap with the single common output, and resulting in *two* gaps for a single sensing element.

3.2. Fabrication of resistive sensor arrays

The microfluidic devices containing a multiplexed resistive sensor array consist of two components, a flexible thin-film polyimide (Kapton 500 HN, DuPont, Wilmington, DE) substrate that supports the sensor array, and a poly(dimethylsiloxane) (PDMS) mold that defines the microfluidic channels. Use of a polyimide film with a very low thermal conductivity (κ_{Kapton} = 0.12 W/m K) promotes heat transfer from the resistor to the surrounding liquid, thereby increasing the sensitivity of the sensors to subtle differences in the TCR of various liquids [26,28,53]. Other techniques exist to insulate resistive sensors without the use of a plastic substrate (such as removing some of the substrate materials directly beneath the resistor) [26,54,55], however, these processes require several additional fabrication steps and typically result in physically weaker sensors.

We patterned the sensors and leads using three standard lift-off procedures (Fig. 2). First, the individual resistors were defined in 0.5-μm thick positive photoresist (Shipley S1805, Rohm & Haas, Philadelphia, PA) and then 80 nm of Ni was deposited by electron-beam evaporation (Temescal FC-1800, BOC Edwards, West Sussex, UK) to form the resistors (Fig. 2a). The excess photoresist and metal was removed by lift-off through sonication in an acetone bath. Nickel was chosen as the metal for the resistors because of its relative chemical inertness, relatively low intrinsic electrical resistivity, and relatively high TCR. This combination of electrical and thermal properties produces the largest possible change in current for a given change in temperature among the metals commonly used in microfabrication (i.e. Au, Cr, Ag, Ti, and Pt). Next, the first set of leads and the common ground were defined, also by lift-off. These leads consisted of a 35-Å thick Ti adhesion layer, followed by 100 nm of Au, and finally an additional 75-Å thick layer of Ti used to render the electrode lead surface more hydrophilic for future processing steps (Fig. 2b).

Before the final lift-off step, a 4-μm thick layer of insulating polymer resin (SU-8 5 negative photoresist, Microchem, Newton, MA) was patterned over the areas of the first set of leads that would intersect with the second set of leads, to electrically insulate the two sets from each other (Fig. 2c). This thickness is a tradeoff between avoiding short circuiting through defects in the insulating layer, and ensuring electrical continuity of the second set of

leads deposited on this uneven electrical substrate. The second set of leads (Fig. 2d) was much thicker than the first set (35-Å Ti, 300-nm Au), facilitated by the use of a thicker resist layer to define the leads (10 μm, Shipley SJR-5740, Rohm & Haas). Also, metal deposition for this final step was done by sputtering (ATC 2000, AJA Int., North Scituate, MA) instead of by evaporation deposition. The more isotropic sputter deposition process ensures continuity of the metal film over the insulating layer. Fig. 3 shows a completed multiplexed resistive sensing substrate before being attached to a PDMS microfluidic mold, which is not pictured in order to aid in the visualization of the sensor array. The network consisted of a T-junction upstream from the sensor array used to generate liquid droplets, leading to a single channel passing over the sensors to be tested.

3.3. Fabrication of capacitive and conductive sensor arrays

The capacitive and conductive sensing arrays were fabricated using essentially identical procedures to those used for the resistive sensors. The sensor elements, first set of leads, and common ground were comprised of evaporated 35-Å Ti, 100-nm Au, and 75-Å Ti patterned by lift-off on a glass slide. An insulating SU-8 layer was then patterned as described above, followed by the sputter deposition of the second set of leads (35-Å Ti, 300-nm Au). Finally, a second 4-μm thick SU-8 insulating layer was patterned over portions of the exposed leads to prevent interference with liquid passing over them during testing. Fig. 4 shows a completed multiplexed capacitive or conductive sensing substrate.

3.4. Characterization of multiplexed sensor arrays

PDMS molds (Sylgard 184, Dow Corning, Midland, MI) containing microfluidic networks were prepared via replica molding, as previously reported [56]. The PDMS mold and the substrate were then aligned and brought into reversible contact using a custom-built four-axis micro-aligner. To prevent leakage during testing, the substrate and mold were clamped together between two clear polycarbonate slabs. Fluid was introduced to the device through a 0.022 in. ID polyethylene tube attached to a syringe. The tubing was inserted into inlet holes in the PDMS that had been punched before the mold was placed on the substrate. The flow rate of the injected fluid was controlled with a syringe pump (model 11, Harvard Apparatus, Holliston, MA).

The performance of the resistive and capacitive sensor arrays was tested by connecting them to a custom-built power supply via a standard 34-pin socket connector. The power supply, controlled by a computer program (LabVIEW 8, National Instruments, Austin, TX), enabled the application of a constant potential between 1 and 100 mV to up to eight different electrical channels, along with the recording of the resulting current through each individual circuit. While each channel had its own electrical lead from the power supply, all eight channels were connected to the same common output electrode to both reduce the number of external electrical contacts necessary for a given sensor array, and to simplify the electronics within the power supply. The system was specifically designed to detect slowly fluctuating current differences on the order of 1 nano-Ampere atop a micro-Ampere baseline current in all eight channels simultaneously.

Data for devices with conductive sensors (which require a constant current power source) was collected using a potentiostat (Autolab PGSTAT30, Eco Chemie, Utrecht, The Netherlands), which allowed only a single individual sensor to be tested at a time. However, with an appropriate multichannel constant current power supply, the performance of arrays of multiplexed conductive sensors could in principle also be tested.

4. Results and discussion

4.1. Performance of individual electrical sensors

4.1.1. Resistive sensors

Fig. 5a depicts data for a device containing a linear series of three resistive sensors spaced 4 mm apart in a 250-μm wide by 100-μm high microchannel. Alternating 5-μL plugs of deionized water in a low thermal conductivity fluorinated solvent (Fluorinert FC-40, 3 M, St. Paul, MN) were flown at a rate of 0.1 mL/h over the resistors, and the current across each was monitored for a constant applied potential of 30 mV. The water plugs were introduced to the FC-40 carrier stream at a T-junction in the microfluidic network upstream from the sensors. Surface tension at the liquid–liquid interface between these two immiscible fluids creates a 2-phase segmented flow: a train of droplets of one fluid (here water) surrounded by the second fluid (fluorinated organic solvent, FC-40) [41,42]. Each water plug activates each sensor sequentially, hence the lag in the current peaks between sensors 1, 2, and 3. The lag corresponds to the time a plug takes to travel the short distance from one sensor to the next, thereby illustrating the high degree of time resolution attainable using the resistive sensors. The data indicates that the plugs are flowing at approximately 0.1 cm/s, which is in good agreement with plug velocities estimated from the syringe pump flow rate. Each increase and decrease in current represents the passage of one plug of water and one plug of FC-40, respectively, over a resistor. The difference in thermal conductivity between water and FC-40 ($\kappa_{water} = 0.6\,W/m\,K$, $\kappa_{FC\text{-}40} = 0.06\,W/m\,K$) leads to the slight upward trend observed in the overall current traces. The heat transfer from the resistor to the water is larger and faster than to the FC-40, resulting in a small net increase in current for each water/FC-40 iteration.

Fig. 5a also demonstrates the resistive sensors' ability to differentiate between different liquid types, not simply between liquids and air. The sensors are effectively measuring changes in the thermal conductivity of the surrounding liquid, which appear as shifts in the slope of the current versus time graph. The larger difference in thermal conductivity from one liquid to another, the larger the change in slope will be. The resistors can therefore be used to distinguish between varying classes of liquids that have significant differences in thermal conductivity ($\kappa_{air} = 0.024\,W/m\,K$, $\kappa_{oils} \approx 0.1\,W/m\,K$, $\kappa_{alcohols} \approx 0.2\,W/m\,K$, $\kappa_{aqueous\ solutions} \approx 0.6\,W/m\,K$), yet are less useful for sensing more discrete differences between similar liquids (i.e. ethanol vs. methanol or salt solutions of varying concentrations).

A key characteristic of a droplet position detection system is the sampling rate at which it can detect. The recovery time of a sensor response signal from its detection value to its baseline will determine how fast a droplet can be moving and still be detected, and also how close together droplets in series can be and still be distinguished form one another. Of the three types of sensors discussed here, the resistive sensors have the slowest response time because their detection mode is based on a relatively slow thermal change in the resistor, whereas the capacitive and conductive sensors rely on much quicker redistribution of electrical charges. From the data presented here, the resistive sensors have a characteristic response of approximately 10 nA/s to the water plugs, and approximately 1 nA/s to the FC-40, rates which are on par with calculated expected values for conductive heat transfer from an insulted heat source. The fluctuation in the data due to noise is on the order of 5 nA, meaning that to detect a water droplet here, the plug must be moving slow enough to be in contact with the resistor for at least 1 s, and the droplets must be spaced at least 5 s apart. For resistive sensor detection, the droplet must actually contact the sensor in order to generate a large enough signal for detection. Therefore, the smallest size droplet the resistive sensors could still detect in

the channels used here is on the order of ~100 nL, to ensure that the droplet still contacts the channel walls. Droplets of this size will still be easily detected at typical microfluidic flow rates in the range of 0.01–1 mL/h, as long as they are spaced by 5 or more seconds at the flow rate used. Resistive sensors will not be suitable for scenarios in which rapidly moving trains of droplets need to be detected.

4.1.2. Capacitive sensors

Fig. 5b demonstrates the induced current principle of a constant potential, coplanar capacitive sensor. Alternating 5-μL plugs of water, air, and ethanol ($\varepsilon_{water} = 80$, $\varepsilon_{air} = 1$, $\varepsilon_{ethanol} = 24$) were allowed to flow at 0.1 mL/h over a single 25-μm gap capacitive sensor in a 250-μm wide by 100-μm high microchannel under an applied potential of 1 V. That the specific values of the induced currents are not identical for both water peaks is a result of the highly transient nature of this induced current behavior, coupled with the resolution limit of the data acquisition system (10 Hz). However, the magnitudes of the signals, and therefore also the specific dielectric constants of the droplets, are not critically important. Since the goal is to easily detect whether or not a droplet is present, the occurrence of a signal is all that matters. A liquid droplet with a dielectric constant different from that of the carrier fluid will always yield a distinct induced current spike when it passes over a capacitive sensor, yet the magnitudes of the signals from varying liquid species are difficult to distinguish in the present detection configuration. A higher sampling rate would enable more precise measurement of the induced current, thus potentially allowing for droplets of different composition being distinguished, provided they are of the same size.

The response time for the capacitive sensors is much faster than that of the resistive sensors. The capacitive data was sampled at a rate of 10 Hz, and each induced current spike was defined by a single data point, meaning that droplets need only be spaced approximately 0.2 s apart to still be distinguished from each other using these sensors. Detection equipment with a faster sampling rate would allow for even finer droplet spacing. Also, the droplets do not necessarily have to contact the sensor surface in the capacitive case, since all that is being measured is the change in dielectric constant over the channel cross-section perpendicular to the sensor. This allows for much smaller droplets to be detected than in the resistive case, on the order of ~100 pL. The capability to detect a high frequency of very small droplets means that the capacitive sensors theoretically can also handle much faster flow rates than resistive sensors (>10 mL/h). Flow rates this high are not practical for most common microfluidic applications, but could potentially allow the capacitive sensors to be used in other areas, such as high throughput particle counters and sorters.

4.1.3. Conductive sensors

Fig. 5c shows a typical response of a conductive sensor in a microchannel. Alternating 5-μL plugs of water, air, and ethanol were passed over a single 20-μm gap conductive sensor in a 250-μm wide by 100-μm high microchannel at 0.1 mL/h, with an imposed constant current of 1 μA. These sensors are essentially on–off switches. When the liquid between the electrodes is nonconductive, the circuit is open. When a conductive liquid fills the gap, the circuit is closed and a potential drop proportional to the conductivity of the liquid is observed. The erratic shape of the ethanol detection peaks is a result of the liquid's extremely low conductivity. The flow of charge through the circuit is so low, that at some points during the detection of an ethanol plug, the measured potential drop becomes nearly undefined, hence the erratic shape of the curves. The conductive sensors are of course unable to detect nonconducting liquids, yet are very sensitive to subtle differences between conductive species. The large, sharp, steady peaks produced by the conductive sensors mean that liquid droplets

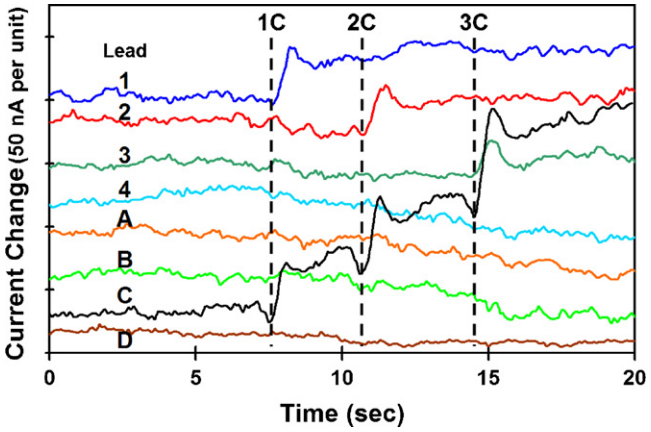

Fig. 6. Detection traces for multiplexed resistive sensing of a 1-μL plug of water passing over sensors 1C, 2C, and 3C in a (1–4) × (A–D) array of sensing elements. Each pair of changes in current that occur at the same time pinpoints the location of the water plug flowing over the specific sensor defined by those two leads. The current for lead C keeps increasing in a stepwise pattern because the amount of time between the trailing edge of the droplet leaving one sensor and the leading edge of the droplet passing over the subsequent sensor is very short and does not allow for the sensor to return to its baseline temperature. The signal threshold value was $\Delta I = 10$ nA.

with wide-ranging conductivity differences thus can easily be distinguished from one another, and preliminary experiments have shown that even electrolyte plugs of small concentration differences ($\Delta C < 1$ M) may be differentiated.

Like the capacitive sensors, the conductive sensors have a much quicker response time than the resistive sensors, because the conductive sensors rely on a rapid change in electrical current rather than a much slower adjustment of a thermal gradient. The sampling rate here was again 10 Hz, corresponding to a droplet-to-droplet spacing of 0.2 s, provided that this time is longer than the residence time of the trailing edge of the leading droplet on the conductive sensor. However, because the droplets being detected must touch the conductive sensor to complete the circuit, the minimum droplet size for the channels used here will be larger than for the capacitive sensors and on par with the resistive sensors, on the order of ~100 nL for the channel dimensions used here.

4.2. Performance of multiplexed resistive sensor arrays

The device shown in Fig. 3 was used to test the multiplexed resistive sensor arrays. A 1-μL water plug was flown through a 250-μm wide by 100-μm high channel over sensors 1C, 2C, and 3C at a flow rate of 2 mL/h (~0.1 cm/s) while a potential of 75 mV was applied to each electrode and the current through each was monitored (Fig. 6). Each concurrent set of peaks indicate that the water plug is flowing over the specific sensor pinpointed by those two electrodes. Fig. 6 clearly shows the system's ability to use electrical sensors to accurately track a discrete plug of liquid throughout a complex two-dimensional microfluidic network while using a minimal number of external electrical connections. The slight drift observed in the current traces of the activated sensors is a result of the large difference in thermal conductivity between water and air. The resistors cool down much faster in the presence of water than heat up in air, and therefore the current traces for the affected electrodes do not immediately return to their baseline values after the plug has completely passed over them.

A reduction in the overall sensitivity of the resistive sensors in these circuit arrays compared to individual resistive sensor circuits is a consequence of the massively parallel nature of the multiplexing design. To compensate for this, the resistors must be designed to maximize their detection capability. The change in current, ΔI, for a

given resistive sensor due to a thermally induced resistance change is related to resistance by

$$\Delta I \sim \frac{R_1 - R_2}{R_1 R_2} \quad (1)$$

where R_1 is the initial resistance of the resistor under the constant applied potential V, and R_2 is the resistance when a liquid droplet is in contact with the resistor. Eq. (1) implies that to increase the measured current change, the initial resistance of each sensor should be lowered. This is somewhat counterintuitive because one might expect that if the initial resistance were increased, so too would the initial temperature of the resistor. That in turn would lead to the conclusion that the larger temperature difference between the resistor and liquid will result in larger changes in resistance, and therefore in larger changes in current as well. However, in this system, the temperature change itself is not important, whereas the *amount of heat*, q, that is removed from the resistor by the liquid, is. This amount of heat is equal to the power, P, dissipated by the resistor, as given in the following equation:

$$q = P = I^2 R \quad (2)$$

Here, the amount of heat absorbed is indeed proportional to the resistance, but is *quadratically* dependent on the current passing through the system, which would be decreased by increasing the initial resistance, according to Ohm's Law. Therefore, any advantage gained by increasing the initial resistance of a resistive sensor will be overshadowed by the negative effect of the reduced current, thus suggesting that the best design for a resistive sensor is one with a counterintuitive *low* initial resistance. The only qualifier to this is that the resistance should be high enough so that the heat produced by the resistor is sufficiently larger than the heat generated by the electrical leads. This can be achieved by fabricating the electrodes out of a highly conductive metal, such as gold, and by patterning them to be as thick and wide as possible. For the devices used here, the width of each individual electrode was 1.65 mm. The serpentine resistors had an overall pathlength of 1.2 mm, a cross-sectional width of 30 μm, and a horizontal and vertical pitch of 5 and 3 mm, respectively.

The size requirements for the resistors and electrodes used here do limit the extent to which the resistive sensors may be densely patterned. Since having resistors with a relatively low initial resistance is desirable, trying to make them as small as microfabrication technology allows is not beneficial. However, the serpentine design does minimize the resistor pattern footprint as much as possible. The limiting factor in the size reduction of the array though, is the width of the electrical leads needed to maintain a sufficiently low contact resistance connection between the power supply and the actual sensors. The resistors are negligible in size compared to the leads. Based upon previous characterization experiments, we estimate that the widths of the leads may be reduced by approximately 25–50% and still allow for acceptable detection peaks, resulting in a sensor density on the order of 1 sensor/mm^2, although three or four sensors could potentially be placed within 1 mm^2, provided the area in proximity of such a sensor array would be available for leads.

When a liquid plug is detected in the multiplexed resistive sensing system, two large peaks pinpointing the position of the plug are prevalent, yet several small decreases in current also appear, a remnant of the interconnectedness of the system. The detection peaks are distinguished from the noise by selecting a threshold value that must be reached before a peak is considered a detection instance. Based upon calibration experiments for this setup where we sought to determine the minimum signal droplets of varying size and composition would yield, the threshold value was set to be $\Delta I = 10$ nA.

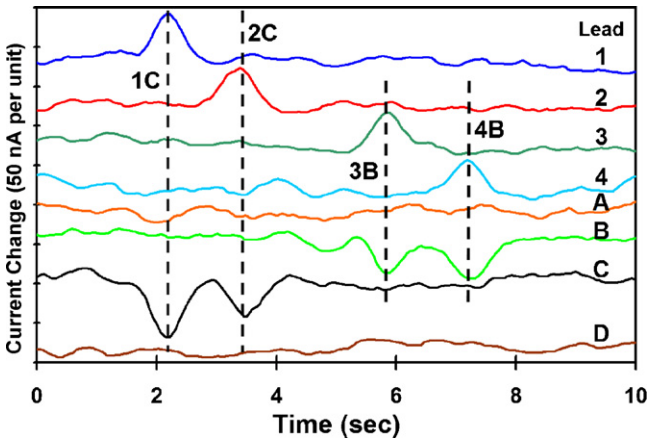

Fig. 7. Detection traces for multiplexed capacitive sensing of a 1-μL plug of water passing over sensors 1C, 2C, 3B, and 4B in a (1–4) × (A–D) array of sensing elements. Each pair of positive and negative current spikes occurring simultaneously represents the water plug passing over the sensor denoted by those particular electrodes. The signal threshold value was $\Delta I = 5$ nA.

Detecting multiple liquid plugs simultaneously could in principle be accomplished by creating an array of sensors where each one has a unique size and shape. These geometric differences will result in differences in the magnitudes of the detection peaks for each sensor. This would allow concurrent detection incidences at, for example, sensors 2B and 3C to be distinguished from sensors 2C and 3B.

4.3. Performance of multiplexed capacitive sensor arrays

To test the capacitive multiplexing system, a 1-μL water plug was flown through a 250-μm wide by 100-μm high channel over sensors 1C, 2C, 3B, and 4B at a flow rate of 1.5 mL/h (~0.1 cm/s) while a constant potential of 100 mV was applied to each electrode (Fig. 7). The data was taken at a rate of 10 Hz and the noise was filtered using a 5-point unweighted moving average [57]. Calibrations performed similar to those in the resistive case resulted in a signal threshold value for these capacitive sensors of $\Delta I = 5$ nA. Each pair of positive and negative current spikes occurring at the same time represents the liquid plug passing over the sensor denoted by those particular electrodes, again illustrating the multiplexing system's ability to track a droplet through a microfluidic network using a minimal number of electrical connections. The positive/negative trend arises from the multiple electrode gaps needed to create the multiplexed capacitive sensor array. The positive current spike always comes from the vertical electrode of the pair, and the negative spike from the horizontal electrode. The two leads interact not only with the common electrode, but also with each other. Therefore, the initial positive charge on the vertical electrode results in a negative charge on the horizontal one.

The placement and orientation of the two sensor gaps is critical. In order to maintain the effectiveness of the multiplexing arrangement, the gaps should be positioned so that a small plug of liquid may activate both sensing circuits at essentially the same time. Additionally, the sensors' electrical leads must be sufficiently isolated from each other so that they themselves do not act as a capacitor and interfere with the rest of the sensing process. For the devices used here, the electrical leads (150 μm) were much narrower than the sensors (1 mm), thereby minimizing any unwanted effects leads in close proximity of each other may have caused. The gap between each lead and the common output was 50 μm, and the sensors had a pitch of 5 mm in both the horizontal and vertical directions. As a final design point, the regions of the electrical leads closest to the sensing elements were designed to inter-

sect the overlaying microfluidic channels as minimally as possible, and were selectively covered with an electrically insulating SU-8 film.

These relatively large capacitive sensors could be scaled down to accommodate much smaller channels and much denser arrays, as long as a high enough sensor width to electrical lead width ratio were maintained (here we used 20:3). The sensing element is simply a small gap separating two coplanar electrodes, and, as opposed to the resistive case, minimizing this sensing element actually improves the resulting detection signals. Using standard microfabrication technology, sensor gaps and electrical leads could easily be made to be less than 10 μm wide, allowing for the width of the overlying channels to be correspondingly reduced in size. These optimizations could therefore theoretically lead to coplanar capacitive (and conductive) sensor arrays with sensor densities on the order of 25 sensors/mm^2.

5. Conclusions

This paper described the design, fabrication, and characterization of a novel multiplexing arrangement that allows for large arrays of electrical sensors integrated with microfluidic networks to be operated by a small number of external electrical leads. This is a very simple solution to a significant problem in microscale sensing, and is an important step towards the overall goal of completely automated microfluidic control architectures. While all three electrical sensors are capable of tracking the position of a discrete liquid element in microfluidic devices, each sensor has specific advantages and disadvantages which render them suitable for different applications.

The most obvious constraint on any of the sensors is that conductivity sensors can only be used to detect electrically conductive liquids. However, within the realm of conductive liquids, conductive sensing has the strongest signals, the largest signal-to-noise ratios, and is the most sensitive to different liquids, when compared to resistive and capacitive sensing, as evidenced by the very large, sharp, and consistent detection peaks seen in Fig. 5c.

From a practical standpoint, coplanar capacitive and conductive sensors are easier to fabricate than resistive ones. Resistive sensors require an additional lift-off step to first pattern the resistors, and use a flexible polyimide sheet as a substrate, which further complicates the microfabrication process. Also, capacitive and conductive sensors can theoretically be scaled down to much smaller length scales than their resistive counterparts. The sensing element in the capacitive and conductive cases is merely a small gap between two coplanar electrodes. This is in contrast to the intricate serpentine pattern used for resistors, which only becomes more difficult to create when critical length scales approach the sub-micron regime.

Resistive sensors have an advantage, however, in distinguishing between different liquids when one or more of them is nonconductive. In such situations, conductive sensors strictly cannot be used, and capacitive sensors are generally less sensitive to different liquid species than are resistive sensors. Fig. 5a shows that resistive sensors can easily differentiate between alternating plugs of water and nonconducting FC-40, whereas the differences in peaks between water and ethanol for capacitive sensors, shown in Fig. 5b, are less pronounced. Conversely, capacitive sensors are more useful for detecting small slugs of a given liquid suspended in a larger carrier stream, when the droplet of interest actually does not contact the sensor surface. Here, the changes in dielectric constant spanning the cross-section of the channel will have much more of an effect on the induced current signal than will changes in thermal conductivity affect a far away resistive sensor.

In sum, for microfluidic systems dealing with only electrically conductive liquids, conductive sensors are the most powerful, because of their large signal strength and relative ease of fabrication. When nonconductive liquids are present, resistive sensors have been shown to be more sensitive than capacitive sensors during plug flow regimes. However, capacitive sensors may be required for systems operating at length scales below which resistive sensors cannot be easily fabricated, or for when slug flow is used, for example in cases where surface contamination by the liquid transported as a slug (surrounded by carrier liquid) is to be avoided.

Acknowledgments

We would like to acknowledge Jim Wentz from the UIUC School of Chemical Sciences Electronics Shop for help with the design and construction of the power supply used in this study, and also undergraduate student Alexander Kniuksta for his preliminary work characterizing the individual resistive sensors. This work was supported by the National Science Foundation under Award DMI-0328162; an NSF NSEC on Nanomanufacturing.

References

[1] M.U. Kopp, A.J. De Mello, A. Manz, Chemical amplification: continuous-flow PCR on a chip, Science 280 (1998) 1046–1048.
[2] N.A. Lacher, K.E. Garrison, R.S. Martin, S.M. Lunte, Microchip capillary electrophoresis/electrochemistry, Electrophoresis 22 (2001) 2526–2536.
[3] S. Gawad, L. Schild, P. Renaud, Micromachined impedance spectroscopy flow cytometer for cell analysis and particle sizing, Lab Chip 1 (2001) 76–82.
[4] T. Thorsen, S.J. Maerkl, S.R. Quake, Microfluidic large-scale integration, Science 298 (2002) 580–584.
[5] E.R. Choban, L.J. Markoski, A. Wieckowski, P.J.A. Kenis, Microfluidic fuel cell based on laminar flow, J. Power Sources 128 (2004) 54–60.
[6] J. Su, M.R. Bringer, R.F. Ismagilov, M. Mrksich, Combining microfluidic networks and peptide arrays for multi-enzyme assays, J. Am. Chem. Soc. 127 (2005) 7280–7281.
[7] L. Li, J.Q. Boedicker, R.F. Ismagilov, Using a multijunction microfluidic device to inject substrate into an array of preformed plugs without cross-contamination: comparing theory and experiments, Anal. Chem. 79 (2007) 2756–2761.
[8] J.-s. Han, Z.-y. Tan, K. Sato, M. Shikida, Three-dimensional interconnect technology on a flexible polyimide film, J. Micromech. Microeng. 14 (2004) 38–48.
[9] K. Swinney, D.J. Bornhop, Detection in capillary electrophoresis, Electrophoresis 21 (2000) 1239–1250.
[10] M.A. Schwarz, P.C. Hauser, Recent developments in detection methods for microfabricated analytical devices, Lab Chip 1 (2001) 1–6.
[11] S. Kulmala, J. Suomi, Current status of modern analytical luminescence methods, Anal. Chim. Acta 500 (2003) 21–69.
[12] E. Verpoorte, Chip vision—optics for microchips, Lab Chip 3 (2003) 42N–52N.
[13] K.B. Mogensen, H. Klank, J.P. Kutter, Recent developments in detection for microfluidic systems, Electrophoresis 25 (2004) 3498–3512.
[14] A.T. Woolley, K. Lao, A.N. Glazer, R.A. Mathies, Capillary electrophoresis chips with integrated electrochemical detection, Anal. Chem. 70 (1998) 684–688.
[15] A. Hilmi, J.H.T. Luong, Electrochemical detectors prepared by electroless deposition for microfabricated electrophoresis chips, Anal. Chem. 72 (2000) 4677–4682.
[16] A.J. Gawron, R.S. Martin, S.M. Lunte, Fabrication and evaluation of a carbon-based dual-electrode detector for poly(dimethylsiloxane) electrophoresis chips, Electrophoresis 22 (2001) 242–248.
[17] N.A. Lacher, S.M. Lunte, R.S. Martin, Development of a microfabricated palladium decoupler/electrochemical detector for microchip capillary electrophoresis using a hybrid glass/poly(dimethylsiloxane) device, Anal. Chem. 76 (2004) 2482–2491.
[18] E.E. Krommenhoek, J.G.E. Gardeniers, J.G. Bomer, X. Li, M. Ottens, G.W.K. vanDedem, M. VanLeeuwen, W.M. vanGulik, L.A.M. vanderWielen, J.J. Heijnen, A. vandenBerg, Integrated electrochemical sensor array for on-line monitoring of yeast fermentations, Anal. Chem. (2007).
[19] R.M. Guijt, E. Baltussen, G. Van der Steen, R.B.M. Schasfoort, S. Schlautmann, H.A.H. Billiet, J. Frank, G.W.K. Van Dedem, A. Van den Berg, New approaches for fabrication of microfluidic capillary electrophoresis devices with on-chip conductivity detection, Electrophoresis 22 (2001) 235–241.
[20] M. Galloway, W. Stryjewski, A. Henry, S.M. Ford, S. Llopis, R.L. McCarley, S.A. Soper, Contact conductivity detection in poly(methyl methacrylate)-based microfluidic devices for analysis of mono- and polyanionic molecules, Anal. Chem. 74 (2002) 2407–2415.
[21] J. Lichtenberg, N.F. de Rooij, E. Verpoorte, A microchip electrophoresis system with integrated in-plane electrodes for contactless conductivity detection, Electrophoresis 23 (2002) 3769–3780.
[22] J. Tanyanyiwa, S. Leuthardt, P.C. Hauser, Conductimetric and potentiometric detection in conventional and microchip capillary electrophoresis, Electrophoresis 23 (2002) 3659–3666.

[23] R. Tantra, A. Manz, Integrated potentiometric detector for use in chip-based flow cells, Anal. Chem. 72 (2000) 2875–2878.
[24] R. Ferrigno, J.N. Lee, X. Jiang, G.M. Whitesides, Potentiometric titrations in a poly(dimethylsiloxane)-based microfluidic device, Anal. Chem. 76 (2004) 2273–2280.
[25] J.J. van Baar, R.J. Wiegerink, T.S.J. Lammerink, G.J.M. Krijnen, M. Elwenspoek, Micromachined structures for thermal measurements of fluid and flow parameters, J. Micromech. Microeng. 11 (2001) 311–318.
[26] J.-s. Han, T. Kadowaki, K. Sato, M. Shikida, Fabrication of thermal-isolation structure for microheater elements applicable to fingerprint sensors, Sens. Actuators A: Phys. A100 (2002) 114–122.
[27] J.J. van Baar, W.A. Verweij, M. Dijkstra, R.J. Wiegerink, T.S.J. Lammerink, G.J.M. Krijnen, M. Elwenspoek, Micromachined two-dimensional resistor arrays for determination of gas parameters, in: Digest of Technical Papers, Transducers'03, International Conference on Solid-State Sensors, Actuators and Microsystems, June 8–12, 2003, Boston, MA, United States, 2003.
[28] J.-s. Han, Z.-y. Tan, K. Sato, M. Shikida, Thermal characterization of micro heater arrays on a polyimide film substrate for fingerprint sensing applications, J. Micromech. Microeng. 15 (2005) 282–289.
[29] O. Berberig, K. Nottmeyer, J. Mizuno, Y. Kanai, T. Kobayashi, The prandtl micro flow sensor (PMFS): a novel silicon diaphragm capacitive sensor for flow-velocity measurement, Sens. Actuators A: Phys. A66 (1998) 93–98.
[30] M.N. Horenstein, J.A. Perreault, T.G. Bifano, Differential capacitive position sensor for planar mems structures with vertical motion, Sens. Actuators A: Phys. A80 (2000) 53–61.
[31] L.L. Sohn, O.A. Saleh, G.R. Facer, A.J. Beavis, R.S. Allan, D.A. Notterman, Capacitance cytometry: measuring biological cells one by one, Proc. Natl. Acad. Sci. 97 (2000) 10687–10690.
[32] J.Z. Chen, A.A. Darhuber, S.M. Troian, S. Wagner, Capacitive sensing of droplets for microfluidic devices based on thermocapillary actuation, Lab Chip 4 (2004) 473–480.
[33] R. Kapon, I. Sagiv, J. Shappir, N. Mazorski, G. Ziv, D. Shahar, Z. Reich, Method to sense single-particle motion using a tapered-gap microcapacitor, Appl. Phys. Lett. 84 (2004) 4277–4279.
[34] W. Olthuis, W. Streekstra, P. Bergveld, Theoretical and experimental determination of cell constants of planar-interdigitated electrolyte conductivity sensors, Sens. Actuators B: Chem. B24 (1995) 252–256.
[35] B.K. Gale, K.D. Caldwell, A.B. Frazier, Electrical conductivity particle detector for use in biological and chemical micro-analysis systems, in: Proceedings of SPIE-The International Society for Optical Engineering, vol. 3515, 1998, pp. 230–241.
[36] V. Haguet, D. Martin, L. Marcon, T. Heim, D. Stievenard, C. Olivier, O. El-Mahdi, O. Melnyk, Combined nanogap nanoparticles nanosensor for electrical detection of biomolecular interactions between polypeptides, Appl. Phys. Lett. 84 (2004) 1213–1215.
[37] J. Collins, A.P. Lee, Microfluidic flow transducer based on the measurement of electrical admittance, Lab Chip 4 (2004) 7–10.
[38] J.D. Beck, L. Shang, M.S. Marcus, R.J. Hamers, Manipulation and real-time electrical detection of individual bacterial cells at electrode junctions: a model for assembly of nanoscale biosystems, Nano Lett. 5 (2005) 777–781.
[39] G. Marchand, C. Delattre, R. Campagnolo, P. Pouteau, F. Ginot, Electrical detection of DNA hybridization based on enzymatic accumulation confined in nanodroplets, Anal. Chem. 77 (2005) 5189–5195.
[40] T. Thorsen, R.W. Roberts, F.H. Arnold, S.R. Quake, Dynamic pattern formation in a vesicle-generating microfluidic device, Phys. Rev. Lett. 86 (2001) 4163–4166.
[41] J.D. Tice, H. Song, A.D. Lyon, R.F. Ismagilov, Formation of droplets and mixing in multiphase microfluidics at low values of the Reynolds and the capillary numbers, Langmuir 19 (2003) 9127–9133.
[42] B. Zheng, J.D. Tice, R.F. Ismagilov, Formation of droplets of alternating composition in microfluidic channels and applications to indexing of concentrations in droplet-based assays, Anal. Chem. 76 (2004) 4977–4982.
[43] S.A. Khan, A. Guenther, M.A. Schmidt, K.F. Jensen, Microfluidic synthesis of colloidal silica, Langmuir 20 (2004) 8604–8611.
[44] N. Srivastava, M.A. Burns, Electronic drop sensing in microfluidic devices: automated operation of a nanoliter viscometer, Lab Chip 6 (2006) 744–751.
[45] Y. Mo, Y. Okawa, K. Inoue, K. Natukawa, Low-voltage and low-power optimization of micro-heater and its on-chip drive circuitry for gas sensor array, Sens. Actuators A: Phys. A100 (2002) 94–101.
[46] C.H. Shen, C. Gau, Heat exchanger fabrication with arrays of sensors and heaters with its micro-scale impingement cooling process analysis and measurements, Sens. Actuators A: Phys. A114 (2004) 154–162.
[47] J.-J. Park, M. Taya, Design of micro-temperature sensor array with thin film thermocouples, J. Electronic Packaging 127 (2005) 286–289.
[48] L. Jiang, W. Man, Y. Zohar, Micromachined polycrystalline thin-film temperature sensors, Meas. Sci. Technol. 10 (1999) 653–664.
[49] K.-D. Song, B.-S. Joo, N.-J. Choi, Y.-S. Lee, S.-M. Lee, J.-S. Huh, D.-D. Lee, A micro hot-wire sensors for gas sensing applications, Sens. Actuators B: Chem. B102 (2004) 1–6.
[50] S. He, M.M. Mench, S. Tadigadapa, Thin film temperature sensor for real-time measurement of electrolyte temperature in a polymer electrolyte fuel cell, Sens. Actuators A: Phys. A125 (2006) 170–177.
[51] W.C. Shin, R.S. Besser, A micromachined thin-film gas flow sensor for microchemical reactors, J. Micromech. Microeng. 16 (2006) 731–741.
[52] C. Ionescu-Zanetti, J.T. Nevill, D. Di Carlo, K.H. Jeong, L.P. Lee, Nanogap capacitors. Sensitivity to sample permittivity changes, J. Appl. Phys. 99 (2006) 024305/1–124305/5.
[53] M. Aslam, C. Gregory, J.V. Hatfield, Polyimide membrane for micro-heated gas sensor array, Sens. Actuators B: Chem. B103 (2004) 153–157.
[54] H.R. Chen, C. Gau, B.T. Dai, M.S. Tsai, A monolithic fabrication process for a micro-flow heat transfer channel suspended over an air layer with arrays of micro-sensors and heaters, Sens. Actuators A: Phys. A108 (2003) 81–85.
[55] D.N. Pagonis, A.G. Nassiopoulou, G. Kaltsas, Porous silicon membranes over cavity for efficient local thermal isolation in situ thermal sensors, J. Electrochem. Soc. 151 (2004) H174–H179.
[56] D. Qin, Y. Xia, G.M. Whitesides, Rapid prototyping of complex structures with feature sizes larger than 20 mm, Adv. Mater. 8 (1996) 917–919.
[57] D.A. Skoog, F.J. Holler, T.A. Nieman, Principles of Instrumental Analysis, 5th ed., Saunders College Publishing, Chicago, 1998, pp. 108–110.

Biographies

M.C. Cole received his MS and PhD degrees in chemical engineering from the University of Illinois. His research focused on the development of sensing and routing platforms for microchemical systems comprised of large arrays of microfluidic channels. In December 2008 he joined the Brady Corporation in Milwaukee, WI.

P.J.A. Kenis received a PhD in chemical engineering from Twente University, The Netherlands and is currently an associate professor of chemical & biomolecular engineering at the University of Illinois with affiliate appointments in the Beckman Institute, the Institute for Genomic Biology, and the department of Mechanical Science & Engineering. His research efforts include the development of microchemical systems: membraneless microfuel cells, microreactors for synthesis, microfluidic chips for pharmaceutical and (membrane) protein crystallization, platforms for biological cell studies (regenerative biology), sensors and valves for integrated microfluidic networks, and micro/nanofluidic tools for nanomanufacturing.